

Supplementary Information: Catastrophic magnetic flux avalanches in NbTiN superconducting resonators

Lukas Nulens^{1*†}, Nicolas Lejeune^{2†}, Joost Caeyers¹, Stefan Marinković², Ivo Cools³, Heleen Dausy¹, Sergey Basov¹, Bart Raes¹, Margriet J. Van Bael¹, Attila Geresdi³, Alejandro V. Silhanek² and Joris Van de Vondel¹

¹*Quantum Solid-State Physics, Department of Physics and Astronomy, KU Leuven, Celestijnenlaan 200D, Leuven, B-3001, Belgium.

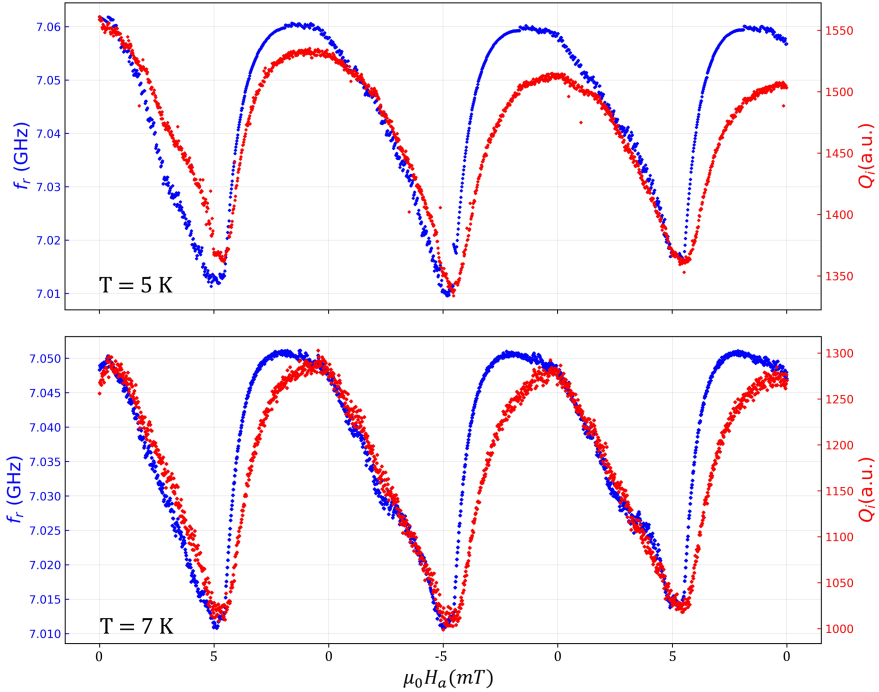
²Experimental Physics of Nanostructured Materials, Q-MAT, CESAM, Université de Liège, Allée du 6 Août 19, Sart Tilman, B-4000, Belgium.

³Quantum Device Physics Laboratory, Department of Microtechnology and Nanoscience, Chalmers University of Technology, Goteborg, Kemivägen 9, SE-412 58, Sweden.

*Corresponding author(s). E-mail(s): lukas.nulens@kuleuven.be
joris.vandevondel@kuleuven.be;

†These authors contributed equally to this work.

1 Supplementary Note 1: Comparison between f_r and Q_i as a function of the applied field ($\mu_0 H_a$).



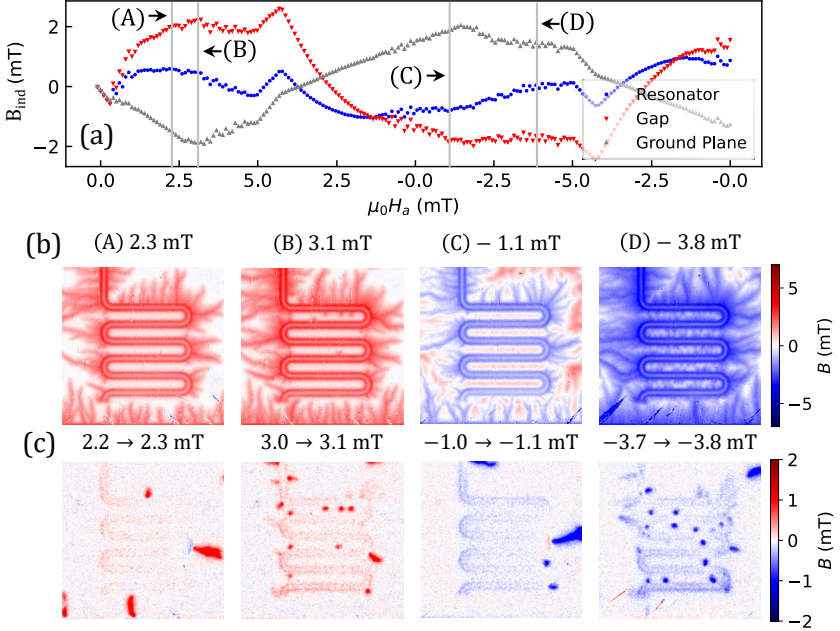
Suppl. Fig. 1 The resonance frequency and internal quality factor as a function of the applied magnetic field $\mu_0 H_a$ indicated in blue and red respectively. The top panel was obtained at $T = 5$ K and the bottom panel at $T = 7$ K. The magnetic field has been swept to complete the following loop $0 \rightarrow 5 \rightarrow -5 \rightarrow 5 \rightarrow 0$ mT.

The upper panel of Suppl. Fig. 1 shows the resonance frequency (blue) and internal quality factor (red) as a function of the applied field at a temperature of $T = 5$ K for the longest resonator. Before the measurement started the sample was field cooled (-0.1 mT) in order to mitigate the remnant field. After this field cool the field was swept as follows: $0 \rightarrow 5 \rightarrow -5 \rightarrow 5 \rightarrow 0$ mT. After every field step the real and imaginary part of the transmission parameter was measured, subsequently, the f_r and Q_i were extracted as described in the main text. A similar measurement at $T = 7$ K is shown in the bottom panel.

2 Supplementary Note 2: Effect of magnetic avalanches in the ground plane delimited by the meander resonator

The upper panel of Suppl. Fig. 2 shows the perpendicular component of the induced field $B_{ind} = B - \mu_0 H_a$ along the line of the resonator (blue dots), in the gap separating the resonator from the ground plane (red triangles) and in the ground plane delimited by the meander of the resonator (grey triangles), as a function of the applied magnetic field at $T = 5$ K. A selected set of magneto-optical images in the region of interest are displayed in the middle row for the applied magnetic fields indicated with label (A-D). The lower row shows differential images obtained by subtracting consecutive applied fields and revealing the magnetic flux invasion activity.

At low applied fields a unique diamagnetic ($B_{ind} < 0$) response is observed for the gap, resonator, and ground plane. This regime corresponds to the magnetic screening produced by Meissner currents circulating mainly at the outer rim of the ground plane. The observed unique response is a consequence of averaging the local field through the meander of the resonators, but does not imply a uniform magnetic field in the resonator. Once a magnetic perforation takes place, the magnetic response of the gap, resonator and ground plane, start to differ from each other. The flux injection into the gap manifests itself as a rapid increase of B_{ind} towards positive values, a fingerprint of flux focusing effect. A somewhat similar trend is observed for the resonator, although we cannot disregard the possibility that the few-pixels-wide region where the local field is estimated along the resonator picks up also signals from the gap. Higher imaging resolution can be implemented to avoid this problem, at expense of proportionally reducing the field of view. Unlike the gap and the resonator, the ground plane continues to exhibit a diamagnetic response all the way up to about $\mu_0 H_a = 3$ mT. The MOI image obtained at point (A) shows that in this region there is indeed little penetration of magnetic field in the ground plane lying inside the meander and all avalanches take place at the outer contour of the resonator (not taken into account in the B_{ind} values plotted in the upper panel). Applying a magnetic field beyond 3 mT show that the absolute value of the local magnetization for the three regions tend to decrease, in other words B approaches the applied field, which is a sign of magnetic pressure relief. Inspecting the magnetic landscape in this region (point (B)) permits to associate the origin of this effect to the development of small magnetic flux avalanches inside the ground plane. The onset of this regime, corresponding to the minimum of B_{ind} for the ground plane, correlates with the kink observed in the $f_r(\mu_0 H_a)$ curve shown in Figure 2 of the manuscript.



Suppl. Fig. 2 Focus on the meander of the longest resonator. (a) The response of the perpendicular component of the induced field of 3 distinct regions of the resonator as a function of the applied field. (b) Background subtracted MOI images at 4 selected magnetic fields emphasising two penetration regimes in the ground plane: at first, the appearance of avalanches on the contour of the resonator, then the penetration of magnetic field through point avalanches inside the meander. (c) Differential MOI images at the same magnetic field values.

After reaching the maximum applied field of 5 mT and starting to decrease the applied field, the critical state profile inverts and $B_{ind}(H_a)$ follows a linear response with similar slope (but opposite sign) to that observed in the Meissner state. This linear regime changes trend once the full critical state profile has been inverted, which manifest itself as a kink (peak) for the ground plane (gap and resonator). Note that no inner avalanche activity is observed in this regime (point (C)). However, continuing to reduce the magnetic field toward negative values eventually leads to the appearance of flux avalanches of opposite polarity inside the meander (point (D)).